Laser-excitation technique for the measurement of absolute transition probabilities of weak atomic lines

H. S. Kwong, Peter L. Smith, and W. H. Parkinson
Harvard-Smithsonian Center for Astrophysics, Cambridge, Massachusetts 02138
(Received 24 August 1981)

A new laser selective-excitation technique for the determination of absolute transition probabilities of weak allowed, intersystem, and forbidden atomic lines has been developed. It exploits the fact that the oscillator strength is proportional to the number of stimulated absorptions and emissions produced by a narrow-band laser pulse of known energy which is in resonance with an atomic transition. The method has been tested by studying the $3s^2\,{}^1S_0$-$3s\,3p\,{}^3P_1^o$ intersystem transition in Mg I. Magnesium vapor was produced in a resistively heated oven and excited with a Nd:YAG laser-pumped dye laser. The lower-level population was monitored with the hook method while the equivalent width of the $^3P^o$-$3s\,4d\,{}^3D$ multiplet was used to determine the $^3P_1^o$ level population, which is equal to the number of stimulation absorptions. A laser-produced plasma was used as a background continuum source. The laser energy was determined with a disk calorimeter. We show that multiphoton, collisional, and power-dependent processes and mode structure in the laser do not affect the measurement. Our result, $A=(2.19\pm0.30)\times10^{+2}$ sec^{-1}, or $f=(2.06\pm0.29)\times10^{-6}$, is in good agreement with theoretical and other experimental data. The technique could be applied to lines several orders of magnitude weaker than the Mg I intersystem line.

I. INTRODUCTION

Absolute radiative transition probabilities (A values)—or oscillator strengths (f values[1])—for intersystem and forbidden lines in atoms are needed to provide information on physical conditions in low-density plasmas. Measured A values can also be used to assess calculated values, and thus, theoretical methods.

A number of techniques have been used for measurements on weak lines. A comprehensive list is not appropriate here; representative examples are presented in Refs. 2—8. These techniques have advantages and disadvantages, making them suitable for a variety of measurements of weak-line transition probabilities. In this paper we present a method that combines laser-selective excitation with standard spectroscopic techniques, which can be used for such measurements on a wide range of atomic species in the vapor phase.

The remainder of the paper is divided into five sections. Section II presents the method and lists the assumptions made in its development. In order to test the method, we have measured the transition probability for the $3s^2\,{}^1S_0$-$3s\,3p\,{}^3P_1^o$ intersystem transition in Mg I. Section III describes this measurement, giving details of the apparatus and considering possible instrumental effects. Section IV presents the data analysis and the results. Section V discusses the assumptions, listed in Sec. II, in the context of the experimental parameters. Section VI consists of a summary.

II. BASIC CONCEPT, ASSUMPTIONS, AND APPROXIMATIONS

If a narrow-band, pulsed laser is tuned into resonance with an atomic line, the number of stimulated emissions and absorptions is proportional to the laser-pulse energy and the oscillator strength of the line. For high, laser-pulse energies and allowed transitions, the two levels connected by the line saturate; i.e., the upper- and lower-level populations are in the ratio of their statistical weights. However, for weaker lines, or lower laser energies, the transition will not saturate and, if the laser energy and the number of atoms induced to absorb or emit can be measured, the f value of the transition can be determined. This paper presents the first discussion and exploitation of this technique to the measurement of weak-line oscillator strengths.

To present the method, we consider a four-level atomic system and define levels $|1\rangle$ and $|2\rangle$ as the lower and upper levels, respectively, of the weak transition for which the oscillator strength

f_{12} is to be measured. Simple examples of such systems are formed by the lower levels of the alkaline earth elements and ions isoelectronic to them (cf. Sec. III A and Fig. 1), but other species with low-lying metastable levels could also be studied.

A pulsed laser induces transitions $|1\rangle \rightarrow |2\rangle$. We consider two of many standard spectroscopic techniques that could be used for measuring the changes in the level populations. Transitions $|1\rangle \rightarrow |3\rangle$ and $|2\rangle \rightarrow |4\rangle$ are used. The oscillator strengths of these transitions, i.e., f_{13} and f_{24}, must be known and Nf, the product of column density and oscillator strength, must be appropriately large. The accuracy of f_{12} is limited by uncertainties in f_{13} and f_{24}.

McIlrath[9] independently suggested a similar technique. Thorne[10] independently proposed a variation which does not require that additional oscillator strengths be known.

We assume that a rate equation can be used to describe the level populations; that second- and higher-order, laser-power-dependent effects can be neglected; that the thermally excited populations of the excited levels are small; that collisional quenching processes may be neglected during the length of the laser pulse, and that $A_{23} << A_{21}$ if $|3\rangle$ is lower in energy than $|2\rangle$. Then, if the atomic vapor is optically thin when exposed to a homogeneous radiation field from a laser at central frequency ν_{12} with bandwidth $\Delta\nu_{12}$, the rate of change of the number density of atoms in the upper state $|2\rangle$ is given by

$$\frac{dn_2}{dt} = \frac{1}{4\pi} \int_{\text{line}} (n_1 B_{12}^I - n_2 B_{21}^I) \times L(\nu) I(\nu,t) d\nu - n_2 A_{21} \ . \quad (1)$$

B_{12}^I and B_{21}^I are the Milne coefficients[11]; $L(\nu)$ is the normalized line-shape function; $I(\nu,t)$ is the spectral radiance of the laser radiation field (in units of energy $\text{cm}^{-2}\,\text{sec}^{-1}\,\text{Hz}^{-1}\,\text{sr}^{-1}$); and A_{21} is the Einstein coefficient for spontaneous emission. B_{12}^I and B_{21}^I are related by $g_1 B_{12}^I = g_2 B_{21}^I$, where the g_i are the statistical weights. Equation (1) is insensitive to the polarization of the laser.

We assume that $I(\nu,t)$ is chosen so that $n_2 << n_1$ at all times; i.e., that the system is far from saturation. $n_1(t)$ is essentially constant with value n_1^0. Therefore the last two terms, representing stimulated and spontaneous radiative decay $|2\rangle \rightarrow |1\rangle$, respectively, can be neglected and

$$n_2(T) = \frac{1}{4\pi} B_{12}^I n_1^0 \times \int_0^T \int_{\text{line}} L(\nu) I(\nu,t) d\nu\, dt \ . \quad (2)$$

If the laser bandwidth is wider than the absorption profile of the line and constant over it, i.e., $I(\nu,t) = I_0(t)$ for $\nu \approx \nu_{12}$, then

$$n_2(T) = \frac{1}{4\pi} B_{12}^I n_1^0 \int_0^T I_0(t) dt \quad (3)$$

$$= \frac{\pi e^2}{mc} n_1^0 f_{12} \frac{1}{h\nu} \int_0^T I_0(t) dt \text{ cgs} \ . \quad (4)$$

If T is greater than the length of the laser pulse, then, from Eq. (4), we see that a measurement of $n_2(T)$, n_1^0, and the laser-pulse energy over the line profile allow the oscillator strength to be determined.

A large number of approximations and assumptions have been made in deriving Eq. (4). They are listed in Table I. Because some of the approximations and assumptions must be discussed in relation to the experimental parameters used and possible instrumental effects, the apparatus, procedure, data analysis, and results are discussed first. The approximations and assumptions are then justified in Sec. V.

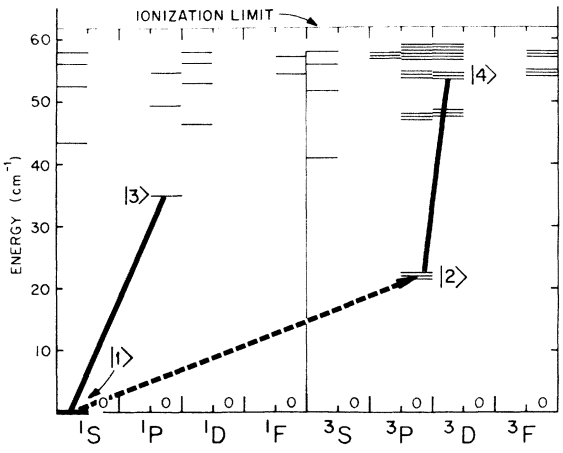

FIG. 1. Partial energy-level diagram for Mg I. Odd-parity levels are those above the o's near lower boundary; other levels have even parity. Levels above 58 000 cm^{-1} are not shown. The levels discussed in the text are numbered $|n\rangle$. $|4\rangle$ includes all levels of the term. The transitions discussed in the text are marked; allowed transitions by solid lines and the intersystem transition for which the f value was measured by a broken line. The $^3P_1^o$ level was pumped with the laser and both the $^3P_1^o \rightarrow {}^3D$ and $^3P_2^o \rightarrow {}^3D$ lines were used to monitor N_2.

TABLE I. Assumptions made in deriving Eq. (4).

	Section
(1) Rate-equation approach is valid	V A
(2) Second- and higher-order, laser-power-dependent effects can be neglected	V B
(3) Thermally excited populations of excited levels are negligible	V I
(4) Collisional populating and depopulating effects are negligible during the laser pulse	V D,E
(5) Spontaneous radiative processes involving $\|2\rangle$, other than $\|2\rangle \rightarrow \|1\rangle$, may be neglected	V J
(6) Atomic vapor is optically thin to laser	V F
(7) Radiation field is homogeneous	V H
(8) $n_2 << n_1$; i.e., system is far from saturation	V H
(9) Laser bandwidth much greater than absorption profile, i.e., $\Delta\nu_L >> \nu_{12}$	V C
(10) Laser has no frequency modes over $\Delta\nu_{12}$, i.e., $I(\nu,t)=I_0(t)$	V G

III. Mg I INTERSYSTEM LINE f VALUE; MEASUREMENT

A. Introduction

In order to test this new method for determining oscillator strengths of weak lines, we have measured the f value for the $3s^2\,{}^1S_0$-$3s\,3p\,{}^3P_1^o$ intersystem line of neutral magnesium (cf. Fig. 1). This line was chosen because its f value has been determined previously[2,3,12] and is of a magnitude appropriate for our present apparatus; i.e., adequate laser power at the desired wavelength and sufficient magnesium vapor column densities could be produced.

B. Measurements of n_1 and n_2

Determination of the oscillator strength f_{12} by this method requires measurement of n_1^0 and $n_2(T)$ [cf. Eq. (4)], which we will abbreviate by n_1 and n_2. Any techniques for measuring number densities could have been employed. We used a Mach-Zehnder interferometer and the hook method[13,14] to measure n_1, while n_2 was determined by measuring an absorption-equivalent width.

C. Apparatus

A schematic diagram of the apparatus is given in Fig. 2. It consists of the components described below.

1. High-power tunable laser

A tunable dye laser system,[15] side pumped by the third harmonic of a Nd:YAG oscillator[16] was tuned to the 457-nm, $3s^2\,{}^1S_0$-$3s\,3p\,{}^3P_1^o$ line of magnesium and used to selectively populate the $^3P^o$ term through the $^3P_1^o$ level. The dye laser was tuned by a grating and beam expander system. The single shot width was 0.0085 nm (12.4 GHz). The time-average width was 0.010 nm (14.4 GHz). These are full width at half maximum (FWHM) values and were measured with a solid etalon, Fabry-Perot interferometer with a 0.014-nm (20-GHz) free spectral range and a measured finesse of 18 at 457 nm. The laser linewidth was about a factor of 5 wider than the Doppler-dominated width of the Mg I line at 800 K; $\Delta\lambda_D=0.0018$ nm ($\Delta\nu_D=2.7$ GHz).

A beam expander and spatial filter were used to produce a homogeneous, collimated beam. The dimension of the laser beam inside the oven (cf. Sec. II B 2) was defined by beam stops of diameter 6.45 mm. The maximum pulse energy passing through the magnesium vapor was about 0.2 mJ, the duration was 7 nsec, and, therefore, the intensity was about 0.1 MW cm^{-2}. The laser-pulse energy was determined with a disk calorimeter[17] before and after each measurement of the f value. Two similar instruments were used. The manufacturer claims accuracy within $\pm 3\%$. Corrections to the measured laser energy were required because of losses, at the additional optical surfaces used to direct the photons into the furnace and at the furnace apertures (cf. Fig. 2), and because part of the

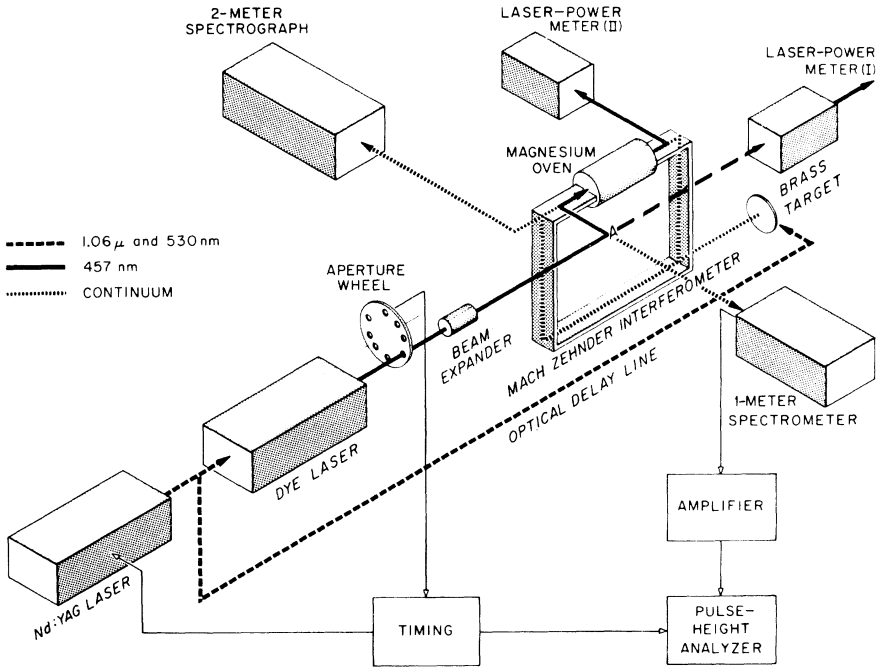

FIG. 2. Schematic diagram of the appartus. Mirrors and beam splitters are not explicitly shown. During the hook-method measurements, the 457-nm radiation was blocked. The beam splitter at A had a reflectivity of 99% at 457 nm and a transmission of about 75% at 309 nm, the wavelength used for the measurement of N_2. For the laser power measurements, this beam splitter was removed and the meter was used in position I. The laser power meter was used at position II when determining the efficiency of the optics used to direct the beam into the furnace. The laser power meter was used in both positions shown, depending upon whether it was being used for calibration or monitoring purposes.

measured output of the laser was continuum radiation. Both corrections were factors of about 0.8; the uncertainty in them was about $\pm 2\%$.

In the derivation of Eq. (4), we assumed that the laser intensity is constant over the absorption line. In practice, however, the laser pulses have modes which vary in frequency and intensity from shot to shot. The method is still valid if a large number of measurements are made and average values of n_2 and laser energy are used (cf. Sec. V H).

2. *Magnesium oven*

A resistively heated furnace was used to provide a source of neutral magnesium vapor. The furnace tube was of 2.5 cm inside diameter. The typical operating temperature was about 800 K; the hot-zone length was 8 cm. The temperature was controlled to within ± 4 K. The ends of the tube were water cooled and had quartz windows. The furnace was loaded with 0.5 to 1 g of magnesium; this amount was adequate for more than 20 h of operation at pressures ranging from 10^{-3} to 10^{-1} Torr. Argon, at a pressure of 5 to 200 Torr, was used as a buffer gas. The beam stop near each end of the heat zone of the oven served to define the overlap of the optical path for the laser and the background continuum probe beams and to restrict the diffusion of magnesium vapor into the cooler end region. n_1 did not change by a detectable amount during the course of a measurement, i.e., during 15 min.

3. *Laser-plasma background continuum*

A laser-produced plasma[18,19] was used as source of background continuum for both the hook and the absorption measurements. This continuum source has a number of desirable features:

(i) It is a point source which can be collimated into a narrow, parallel beam to assure complete overlap of the column of laser-excited atoms and the background continuum probe beam.

(ii) There is no timing jitter; delay can be

achieved by path difference.

(iii) It produces no electrical noise.

(iv) The integrated intensity of emission over a narrow band (e.g., $\Delta\lambda=0.03$ nm) is highly reproducible. The distribution of intensities had a FWHM of less than 5%.

(v) The wavelength range of the emission, which consists of both lines and continuum, can be varied from the vuv to the visible by changing the target material.

The plasma was produced by focusing the unused, first- and second-harmonic, laser radiation from the Nd:YAG laser onto a slowly rotating brass target. The rise time of the emission was about 50 nsec; the fall time about 250 nsec. The optical delay line produced a 30-nsec delay between the laser pulse which excited the atoms from $|1\rangle$ to $|2\rangle$ and the start of the continuum pulse which probed the population of the latter level. The delay ensured that mixing collisions produced thermal populations in the levels of the $^3P^o$ term (cf. Sec. V D). The plasma emission was collected by an f/2 quartz lens and collimated by a telescope. The probe beam was coaxial and opposite in direction to the laser beam (cf. Fig. 2).

4. *Apparatus for measuring n_2*

A 1-m, Czerny-Turner spectrometer equipped with a photomultiplier wired for pulse operation was used to measure the absorption-equivalent width. The spectrometer entrance and exit slits were 22.0 and 40.0 μm, respectively, with an uncertainty of $\pm 1\%$. The spectrometer was tuned to one of the lines of the $3p\ ^3P^o$-$4d\ ^3D$ multiplet. Lines to the different ^3D levels were not resolved but both the $^3P_2^o \rightarrow {}^3D$ and $^3P_1^o \rightarrow {}^3D$ lines, at 309.778 and 309.388 nm, were used in order to ensure that mixing among the levels of the lower term was complete. The oscillator strength of both lines is 0.13. This value was obtained from the lifetime data of Kwiatkowski *et al.*[20] and by using multiplet f-value data of Victor *et al.*[21] to obtain the branching ratios. Kwiatkowski *et al.* state an experimental uncertainty of about $\pm 6\%$.

The output of the photomultiplier was integrated and amplified; the signal was stored and displayed in a pulse-height analyzer. Linearity of this data acquisition system was checked by using neutral density filters to attenuate the plasma emission intensity. Deviations from linearity were less than 1%.

An aperture wheel was used to trigger the Nd:YAG laser and to block every second pulse from the dye laser. Thus, successive signals, denoted J and J_0, respectively, indicated the transmission of the optical system with and without atoms in level $|2\rangle$. The two groups of signals, each containing about 900 measurements, were stored in different halves of the memory of the pulse-height analyzer.

5. *Hook-method apparatus*

The 2-m Littrow spectrograph and Mach-Zehnder interferometer described by Huber and Parkinson[22] were employed for the hook-method[12,13] measurements of n_1. The anomalous dispersion near the $3s^2\ ^1S_0$-$3s\,3p\ ^1P_0^o$ line at 285.213 nm was studied. This has an f value of 1.84, with an uncertainty which we estimate to be of $\pm 5\%$.[23] The spectrograph slit width was 20 μm; 3000 shots were adequate to expose the film.

The measurements of n_1 required removal of the mirrors that were used to direct the background continuum into the spectrometer for the measurements of n_2 (cf. Fig. 2). Consequently, n_1 and n_2 could not be measured simultaneously. However, n_1 varied very slowly (cf. Sec. III C 2) and measurements at 10 to 15 min intervals were adequate for accurate determination of n_1.

IV. DATA ANALYSIS AND RESULTS

A. Determination of f_{12}

N_1, the column density of atoms in level $|1\rangle$, is related to Δ_{13}, the hook separations on the spectrally dispersed inteferograms by

$$N_1=\frac{\pi K(\Delta_{13})^2}{r_0(\lambda_{13})^3 f_{13}}\ , \tag{5}$$

where K is the hook-method parameter, which can be measured on the interferograms (cf. Ref. 13), $r_0=e^2/mc^2=2.82\times10^{-13}$ cm, λ_{13} is the wavelength of the transition $|1\rangle\rightarrow|3\rangle$, i.e., 285.213 nm, and f_{13} is its oscillator strength (cf. Sec. III C 5).

K and the hook separations were read with a comparator. N_1 ranged from about 7×10^{14} cm^{-2} to about 5×10^{15} cm^{-2}. The uncertainty in its determination is about $\pm 8\%$.

Collisional mixing among the levels of the $^3P^o$ term distributes the excited atoms. N_2^j was determined for $j=1$ or 2 by measurement of the

absorption-equivalent width combined with the curve-of-growth technique. A Boltzmann distribution of level populations was observed. The distributions of signals in the two halves of the pulse-height analyzer (cf. Sec. III C 4) had profiles that were roughly Gaussian. The fractional uncertainty in the mean values of the signals, $\bar{J}$, was about ± 0.001. The fractional decrease in intensity $(\bar{J}_0 - \bar{J})/\bar{J}_0$ was typically 0.025. The uncertainty in the absorption measurements is, therefore, about $\pm 6\%$ (one standard deviation).

The equivalent width is related to the two measured intensities by

$$W = SDC\left[\frac{\bar{J}_0 - \bar{J}}{\bar{J}_0}\right]. \tag{6}$$

S, the exit slit width, was 40 μm with an uncertainty of ± 1 μm. D, the spectrometer plate factor, was 0.77 nm/mm. C is a correction factor which accounts for the fact that, when making an equivalent width measurement with a fixed wavelength spectrometer rather than with a scanning instrument, parts of the profile may extend the opening of the exit slit. In our case, where the instrument profile width is much larger than the absorption line width, C can be determined by observing an emission line with various slit sizes. We had $C = 1.88$ with an uncertainty of $\pm 2\%$.

Direct numerical integration over the Voigt function was used to determine the column density N_2^j. The damping constant ranged from about 0.1 to 3, depending upon the buffer-gas pressure. At the column densities used, the deviation from the weak-line (linear) portion of the curve of growth was less than 5%.

The laser energy E, measured by the power meter and corrected in the manner described in Sec. III B 1, is related to the laser spectral radiance where α is the cross-sectional area of the beam. Only the radiance at line center $I_0(t)$ is needed [cf. Eq. (4)]. Because the Fabry-Perot interferograms showed that $I(\nu,t)$ was roughly Gaussian in shape with a FWHM, $\Delta\nu_{1/2}$, of 0.010 nm, we approximated $I(\nu,t)$ by this shape and obtained

$$\int_0^T I_0(t)dt = \frac{E}{\alpha\sqrt{\pi \ln 2 \Delta\nu_{1/2}}}. \tag{7}$$

The uncertainty introduced by this approximation is estimated to be 5%.

Thirteen measurements of f_{12} were made; giving $f_{12} = 2.06 \times 10^{-6}$, with a random uncertainty of $\pm 10\%$, or $A = (2.19 \pm 0.22) \times 10^2$ sec^{-1}. No discernible dependence upon laser energy, buffer-gas pressure, or N_1 was seen (cf. Fig. 3), except for a possible dependence on N_1 at high densities. In one case, at $N_1 = 1.5 \times 10^{16}$ cm^{-2}, a value $f_{12} = 1.5 \times 10^{-6}$ was obtained. We attribute this low value to the fact that the vapor was no longer transparent to the laser beam at these column densities. This low result was not included in the determination of the mean.

B. Uncertainties

The uncertainties associated with the various parameters involved in the data analysis and those stemming from the assumptions and approximations are listed in Table II. Combining the uncertainties in quadrature gives $\pm 15\%$. If the uncertainties in f_{13} and f_{24} are not included, the actual accuracy of the method is shown to be within $\pm 13\%$.

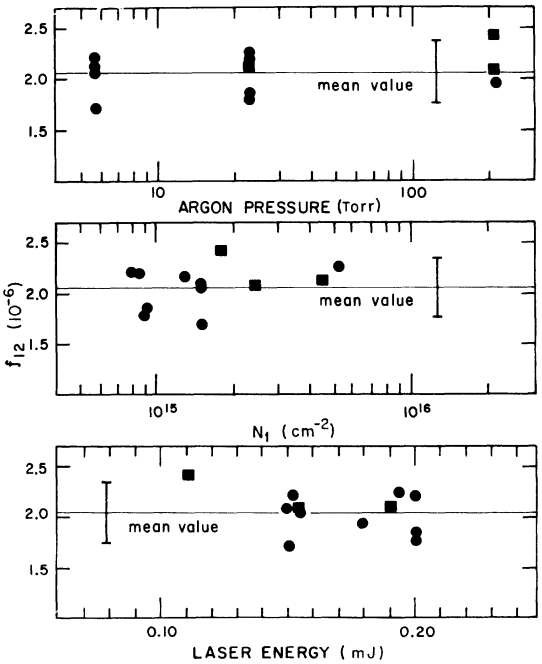

FIG. 3. Dependence of f_{12} on buffer-gas pressure, magnesium-atom density, and laser energy. Squares and circles mark data for which the $^3P_1^o \rightarrow {}^3D$ and $^3P_2^o \rightarrow {}^3D$ lines, respectively, were used to determine N_2. The mean value is shown by the horizontal line. The estimated experimental uncertainty for an individual measurement is shown.

TABLE II. Uncertainties.

Comment	Parameter	Uncertainty (%)
Determination of N_1	$(\Delta_{13})^2$	2×3
	f_{13}	5
	K	1
Determination of W_{24}	S	2.5
	D	2
	C	2
	$\bar{J}_0$, $\bar{J}$	6
Determination of N_2 from W	f_{24}	6
Determination of $\int I_0(t)dt$	E	4.5
	$\Delta\nu_{1/2}$	3
Assumptions and approximations in Table I		0
Approximation of $I_0(\nu,t)$ by Gaussian-Voigt profile fitting		5
		1
	Total	$\pm15\%$

TABLE III. Comparison with other data.

Authors	A (10^2 sec^{-1})	f (10^{-6})	Note
Boldt (1958)[a]	5.2±1	4.9±1	Experiment
Garstang (1962)[b]	2.4 ±0.2	2.26±0.2	Theory
Warner (1968)[c]	1.8 ±0.3	1.69±0.3	Theory
Mitchell (1975)[d]	2.66±0.9	2.5 ±0.8	Experiment
Furcinitti *et al.* (1975)[e]	2.2 ±0.3	2.1 ±0.3	Experiment
Guisfredi *et al.* (1975)[f]	4.2 ±0.4	3.9 ±0.4	Experiment
Laughlin, Victor (1979)[g]	2.17±0.2	2.04±0.2	Theory
This work	2.19±0.30	2.06±0.29	Experiment

[a]Reference 24.
[b]Reference 53.
[c]Reference 54.
[d]Mitchell (Ref. 3) normalized his intersystem line f value to a value of 1.72 for the $3s^3\,{}^1S_0$-$3s3p\,{}^1P^o$ line. We have scaled his result by 1.84/1.72=1.07 (cf. Sec. III B 5).
[e]Reference 2; a remeasurement of the work in Ref. 49 to correct for quenching by contaminants.
[f]Reference 25.
[g]Reference 12.

C. Comparison with other data

Our result, $A = 219 \pm 30$ sec^{-1}, is in good agreement with most of the other oscillator-strength data for the intersystem line of Mg I listed in Table III. The measurement by Boldt[24] and the electron-excited beam measurement of Guisfredi *et al.*[25] yield lifetimes shorter than would be inferred from our result.

V. DISCUSSION OF ASSUMPTIONS AND APPROXIMATIONS

The assumptions and approximations involved in this method for measurement of weak-line transition probabilities are introduced in Sec. II B and listed in Table I. In this section we discuss them in the context of the experimental parameters.

A. Validity of the rate-equation approach

The density-matrix formulation provides a statistical description of the interaction of an atomic gas and an intense, coherent electromagnetic field such as the single or multimode output of a laser.[26,27] This formulation can be reduced to a simple rate equation when the off-diagonal elements of the density matrix vanish. However, the rate equation describes only the population distribution among states; incoherence of the atom ensemble must exist *a priori*.

The pulsed laser used in the current study has a wide spectral width and a short pulse duration. It can hardly be characterized as a coherent radiation source.[28] The atom ensemble prepared by this radiation field is, therefore, relatively incoherent. Further incoherence among the atom ensemble can be introduced by dephasing collisions with buffer-gas atoms. The typical dephasing cross section is about 4×10^{-14} cm^2.[29] The dephasing rate at the buffer-gas pressure used in our measurement is in excess of 10^{10} sec^{-1} at 200 Torr and about 10^9 sec^{-1} at 5 Torr. No dependence on the buffer gas has been observed. Dephasing among the atom ensemble can further be achieved by the finite motion of the atoms in the radiation field[30] and the spatial nonuniformity of the field strength E.[31] The dephasing rate introduced by the above mechanisms favors the vanishing of the off-diagonal matrix elements.

In addition, the rate-equation approach is particularly applicable when the magnitude of the tipping angle θ is much less than π.[32] This condition can readily be achieved by a weak pulse of coherent or incoherent light for a strong transition[32] or a strong pulse of coherent or incoherent light for weak transition where, in both cases, the ground-state population is not significantly perturbed. The value of the tipping angle estimated for our system is more than an order of magnitude smaller than π. Therefore, the rate-equation approach is adequate to describe the interaction between the radiation field and the atom ensemble in our method.

B. Neglect of second- and higher-order, laser-power-dependent effects

The major second- and higher-order effects which must be considered are self-induced transparency, multiphoton excitation and ionization, ionization by laser-induced electron heating, self-focusing and -defocusing, and power broadening.

1. Self-induced transparency

Two of the requirements for the propagation of the 2π pulse—self-induced transparency[33]—are the following: (i) a definite phase relationship among the atom ensemble induced by the radiation field during the excitation period, and (ii) the tipping angle θ must be greater than 2π. Because of the strong dephasing induced by the mechanisms discussed in the preceding section and because θ is more than an order of magnitude smaller than the 2π threshold, self-induced transparency is not expected to occur.

2. Multiphoton excitation and ionization

Changes in populations of $|1\rangle$ and $|2\rangle$ can be brought about by multiphoton processes.[34,35] However, no other levels are found to be in resonance with single- or two-photon transitions from $|1\rangle$ or a single-photon transition from $|2\rangle$. The closest level is the $3s\,4s\ ^1S_0$ at 43 503.3 cm^{-1}. The $3s\,3p\ ^3P_1^o$-$3s\,4s\ ^1S_0$ transition oscillator strength is an order of magnitude less than that being studied.[36] No multiphoton process cross sections for Mg I are available, but, by using the data of Bebb[37] for alkali elements, we estimate that such processes are negligible in our experiment.

3. *Laser-induced electron heating*

Laser-induced ionization by electron heating has been discussed by Measures *et al.*,[38] and observed by Lucatorto and McIlrath,[39] Skinner,[40] and Bachor and Kock.[41] The process requires a long (i.e., several hundred nanoseconds or more) laser pulse so that the laser energy can be efficiently coupled into the atomic vapor. The pulse duration of our laser is relatively short ($\sim$7 nsec) and the ^1S-$^3P^o$ intersystem transition is not saturated. Therefore, we expect that this process is insignificant in our study.

4. *Self-focusing and -defocusing*

We have assumed that the laser energy is uniformly deposited into a well-defined column of magnesium vapor by a carefully collimated laser beam. However, self-focusing or -defocusing of such a beam can occur if the anomalous dispersion of the medium is intensity dependent.[42,43] Self-focusing of laser radiation near an atomic resonance transition has been observed with a laser intensity of about 1 MW cm^{-2}.[44] However, because we are concerned with a weak intersystem transition, self-focusing and -defocusing will be negligible.

5. *Power broadening*

We have considered only a laser bandwidth several times wider than the absorption linewidth. If the absorption linewidth or profile are significantly altered from the above condition, Eq. (4) is still valid but the data analysis becomes complex.

Broadening and shifting of spectral lines by intense, pulsed laser radiation have been reported.[45,46] In the presence of a nonresonant field, the spectral line will be shifted. However, in a resonant field, the line will be split into components and shifted symmetrically with respect to the unperturbed line position.[47]

Bonch-Bruevich *et al.*[48] studied shifting and splitting of the potassium D lines at laser intensity of 10 kW/cm^2. Comparison of their atomic and experimental parameters with those in our measurement shows that these shifting and splitting effects may be neglected.

C. Laser bandwidth much greater than the absorption width, i.e., $\Delta\nu_L >> \Delta\nu_{12}$

The remaining significant broadening mechanisms are Holtsmark broadening, Doppler broadening, and pressure broadening. The magnesium number density is kept at or below 5×10^{15} cm^{-3} so Holtsmark broadening is negligible. The typical Doppler width for the intercombination line is less than 0.018 Å; this is more than five times smaller than the time-average laser linewidth. At maximum buffer-gas pressure of 200 Torr, the Lorentzian width is less than half of the laser linewidth. Above this buffer-gas pressure, the linewidth is too broad to allow us to assume the time-average laser line profile is constant over the absorption line.

D. Collisional populating and depopulating

The $^3P_1^o$ level is selectively populated by the laser. Rapid collisional mixing populates the nearby $^3P_0^o$ and $^3P_2^o$ levels. A thermal distribution of population is achieved in the 30-nsec interval between excitation of $^3P_1^o$ and determination of n_2 (cf. Sec. III C 4).

Collision-induced quenching of the metastable levels by the argon buffer gas or possible impurity gas molecules such as N_2 and O_2 could significantly reduce the population density of the metastable levels.[49] The quenching cross sections of the $^3P^o$ term by rare gases or molecular gases such as N_2 extrapolated from the work of Wright *et al.*[50] are about 10^{-23} and 10^{-18} cm^2, respectively. On the time scale of less than 1 μsec in which the atoms are prepared in their $^3P^o$ term and the measurement is made, quenching due to argon buffer gas and the contaminants is insignificant. This is confirmed by the plot of f value vs argon pressure shown in Fig. 3.

E. Collision-induced absorption

Collision-induced absorption can provide competing channels to populate the metastable levels. The physics of collision-induced absorption and redistribution has been discussed in some detail by Carlsten *et al.*[51] and Cooper.[52] Since collision-

induced absorption involves pseudomolecule formation, it is sensitive to the density of both the ground-state Mg atom and the perturber atom. Our study shows that the f value measured is invariant to number density of both Ar and Mg over an order of magnitude and suggests the insignificance of this effect.

F. Atomic vapor is optically thin to the laser radiation

Throughout our discussion, the laser spectral radiance I is assumed to be constant over the length of the absorbing column. This condition can be approximated by keeping the absorbing medium optically thin at the laser wavelength. In our measurement, the ground-state magnesium column density is kept at a value less than 10^{16} cm^{-2} where the approximation is still valid. Figure 3 shows the plot of the f value as a function of ground-state column density. The measured f values appear to deviate from the mean value when the ground-state column density exceeds 10^{16} cm^{-2}.

G. Laser has no spectral modes over $\Delta\nu_{12}$

We have assumed that the laser bandwidth is wider than the absorption line profile and constant over it. However, mode structure (individual mode width $\simeq$0.0010 nm with mode spacing $\simeq$0.0015 nm) is evident in our dye-laser output even though modes are not resolved. Single-shot linewidth is observed to be 0.0085 nm, but the shot-to-shot laser jitter, which is believed to be caused by thermal effects in the dye solution, gives a time-average linewidth of 0.010 nm. It can be shown, however, that Eq. (4) is still valid when the metastable column density $n_2(T)$ and the laser spectral radiance $I_0(t)$ are replaced by their mean values $\bar{n}_2(t)$ and $\bar{I}_0(t)$.

H. Radiation field is homogeneous and the system is far from saturation; $n_2 << n_1$

The output of our tunable dye laser exhibits spatial inhomogeneity. The spectral radiance at a hot spot could be sufficient to saturate the $^1S_0$-$^3P_1^o$ transition, which would then invalidate Eq. (4). A beam expander ($\times 5$) has been incorporated into our system to eliminate the hot spot and to collimate the beam.

The ratio of n_2/n_1 monitored in all our measurements is less than 0.3%. However, in view of the fact that spectral-mode structure is present in our dye laser output, the condition that $n_1 << n_2$ is not sufficient to guarantee that the transition is far from saturation within the absorption band. The laser spectral modes can induce hole burning in the inhomogeneous-broadened absorption-line profile. For $\Delta\lambda < \Delta\lambda_D$, where $\Delta\lambda$ is the mode spacing of the laser output, a more appropriate requirement to ensure nonsaturation is $n_2 << n_1 \delta\lambda/\Delta\lambda$ where $\delta\lambda$ is the width of the individual laser spectral mode. In our study, the ratio $\delta\lambda/\Delta\lambda$ is close to unity. The nonsaturation condition is therefore satisfied.

I. Thermally excited populations of excited levels are negligible

The typical oven temperature is 800 K and, at this temperature, the thermally excited population of the metastable term is negligible.

J. Spontaneous radiative processes involving $|2\rangle$, other than $|2\rangle \rightarrow |1\rangle$ may be neglected

Each of the fine-structure levels in the $^3P^o$ term is connected to the ground state $^1S_0$ by a radiative transition. However, the transition probabilities of $^3P^o_{0,2}$ are several orders of magnitude smaller than that of the corresponding $^3P^o_1$ level. Depopulation of this level through stepwise fluorescence can be ignored.

VI. SUMMARY DISCUSSION

We have presented a new technique for the measurement of transition probabilities for weak allowed, intersystem, and forbidden lines. As a test of the new method, we have studied the $3s^2\,{}^1S_0$-$3s\,3p\,{}^3P_1^o$ intersystem line of Mg I. Our result,

$$A = (2.19 \pm 0.30) \times 10^{+2}\ \text{sec}^{-1},$$

or

$$f = (2.06 \pm 0.29) \times 10^{-6},$$

is in good agreement with theoretical and other experimental data. This agreement and the estimated measurement uncertainty of $\pm$15%, demonstrate the utility of the method.

This technique could be usefully applied to lines several orders of magnitude weaker if a more powerful laser were used. In fact, the original analysis of this approach was based on the beryllium 455 nm ($2s^2\,{}^1S$-$2s\,3p\,{}^3P^o_1$) intersystem line where the A value is close to three orders of magnitude smaller than the one measured here. The measurement of the Be-line A value is underway.

We have pointed out in Sec. V that there are several parasitic and competing mechanisms that can limit the applicability of the method. The upper limit, therefore, is primarily determined by the dominance of any one of these effects. We expect that this technique is applicable to the measurement of atomic A values $\geq 10^{-2}$ sec^{-1} [$f = O(10^{-11})$].

ACKNOWLEDGMENTS

The authors acknowledge the advice and comments of T. J. McIlrath and A. P. Thorne who independently suggest this method of measuring weak-line oscillator strengths and who provided helpful advice and comments. We thank J. H. Black, J. L. Carlsten, L. D. Gardner, C. Kittrell, D. E. Pritchard, and G. A. Victor for their assistance; N. Galluccio and D. Smith for their technical support. This work was supported in part by NASA Grants Nos. NSG 7176 and NGL 22-007-006, and by the Smithsonian Astrophysical Observatory.

---

[1] $$f_{12} = \frac{mc}{8\pi^2 e^2}\lambda^2 \frac{g_2}{g_1} A_{21} = 1.499\times 10^{-16}\frac{g_2}{g_1} A_{21}\ [\lambda(\text{in Å})]^2 ,$$

where 1 and 2 refer to the lower and upper level, respectively; m, c, and e have the usual meaning; and the g's are the statistical weights of the levels.

[2] P. S. Furcinitti, J. J. Wright, and L. C. Balling, Phys. Rev. A 12, 1123 (1975).

[3] C. J. Mitchell, J. Phys. B 8, 25 (1975).

[4] J. Nilsen and J. Marling, J. Quant. Spectrosc. Radiat. Transfer 20, 327 (1978).

[5] M. C. E. Huber and E. F. Tubbs, Astrophys. J. 177, 847 (1972).

[6] D. E. Blackwell, P. A. Ibbetson, A. D. Petford, and M. J. Shallis, Mon. Not. R. Astron. Soc. 186, 633 (1979).

[7] J. A. Kernahan and P. H. L. Pang, Can. J. Phys. 53, 455 (1975); 53, 1114 (1975).

[8] R. D. Knight and M. H. Prior, Phys. Rev. A 21, 179 (1980).

[9] T. J. McIlrath (personal communication, 1979).

[10] A. P. Thorne (personal communication, 1979).

[11] Quantum absorption and emission coefficients defined in terms of isotropic intensity rather than in terms of the energy density as done by Einstein.

[12] C. Laughlin and G. A. Victor, Astrophys. J. 234, 407 (1979).

[13] W. C. Marlow, App. Opt. 6, 1715 (1967).

[14] M. C. E. Huber, in *Modern Optical Methods in Gas Dynamic Research*, edited by D. Dosanjh (Plenum, New York, 1971), pp. 85–112.

[15] Quanta Ray laser PDL-1.

[16] Quanta Ray die laser DCR-1.

[17] Scientech energy meter 38-1010.

[18] C. G. Mahajan, E. A. M. Baker, and D. D. Burgess, Opt. Lett. 4, 283 (1979).

[19] P. K. Carroll, E. T. Kennedy, and G. O. Sullivan, Appl. Opt. 19, 1454 (1980).

[20] M. Kwiatkowski, V. Teppner, and P. Zimmermann, Z. Phys. A 294, 109 (1980).

[21] G. A. Victor, R. F. Stewart, and C. Laughlin, Astrophys. J. Suppl. Ser. 31, 237 (1976).

[22] M. C. E. Huber and W. H. Parkinson, Astrophys. J. 172, 229 (1972).

[23] P. M. Kelly and M. S. Mathur, Can. J. Phys. 56, 1422 (1978).

[24] G. Boldt, Z. Phys. 150, 205 (1958).

[25] G. Giusfredi, P. Mimquzzi, F. Strumia, and M. Tonelli, Z. Phys. A 274, 279 (1975).

[26] T. J. McIlrath and J. L. Carlsten, Phys. Rev. A 6, 1092 (1972).

[27] J. W. Daily, Appl. Opt. 16, 2322 (1977).

[28] M. Sargent III, M. O. Scully, and W. E. Lamb, Jr., Appl. Opt. 9, 2423 (1970).

[29] S. Asaka, H. Yamada, M. Fujita, and M. Matsuoka, Fifth International Conference on Laser Spectroscopy, June, 1981, Jasper, Alberta, Canada (unpublished).

[30] A. Corney, *Atomic and Laser Spectroscopy* (Clarendon, Oxford, 1977), p. 498.

[31] E. L. Hahn, Phys. Rev. 80, 580 (1950).

[32] C. K. N. Patel and R. E. Slusher, Phys. Rev. Lett. 19, 1019 (1967); S. L. McCall and E. L. Hahn, *ibid.* 18, 908 (1967).

[33] S. L. McCall and E. L. Hahn, Phys. Rev. 183, 183 (1969).

[34] P. Lambropoulos, Appl. Opt. 19, 3926 (1980).

[35] P. Esherick, J. A. Armstrong, R. W. Dreyfus, and J. J. Wynne, Phys. Rev. Lett. 36, 1296 (1976).

[36] C. Laughlin and G. A. Victor, Astrophys. J. 192, 551 (1974).

[37] H. B. Bebb, Phys. Rev. 153, 23 (1967); 149, 25 (1966).

[38] R. M. Measures, N. Drewell, and P. Cardinal, J. Appl. Phys. 50, 2662 (1979).

[39]T. B. Lucatorto and T. J. McIlrath, Appl. Opt. 19, 3948 (1980).
[40]C. H. Skinner, J. Phys. B 13, 55 (1980).
[41]H.-A. Bachor and M. Kock, J. Phys. B 13, L369 (1980).
[42]R. Y. Chiao, E. Garmire, and C. H. Townes, Phys. Rev. Lett. 13, 479 (1964).
[43]P. L. Kelley, Phys. Rev. Lett. 15, 1005 (1965).
[44]D. Grischkowsky and J. A. Armstrong, Phys. Rev. A 6, 1566 (1972).
[45]M. Crance, J. Phys. B 11, 1931 (1978).
[46]Y. Gontier and M. Trahin, J. Phys. B 11, L131 (1978).
[47]I. I. Sobel'man, *Introduction to the Theory of Atomic Spectra* (Fizmalgiz, 1963), p. 376.
[48]A. M. Bonch-Bruevich, N. N. Kostin, V. A. Khodovoi, and V. V. Khromov, Zh. Eksp. Teor. Fiz. 56, 144 (1969) [Soviet Phys.—JETP 29, 82 (1969)].
[49]Ultra pure (grade 5) argon was used as the buffer gas. It was supplied by Airco Industrial Gases.
[50]J. J. Wright, J. F. Dawson, and L. C. Balling, Phys. Rev. A 9, 83 (1974).
[51]J. L. Carlsten *et al.*, Phys. Rev. A 15, 1029 (1977).
[52]J. Cooper, in *Laser Physics,* edited by D. F. Walls and J. D. Harvey (Academic, New York, 1980).
[53]R. H. Garstang, J. Opt. Soc. Am. 52, 845 (1962).
[54]B. Warner, Mon. Not. R. Astron. Soc. 140, 53 (1968).